ACS OMEGA

http://pubs.acs.org/journal/acsodf

Article

Sequential Injection Analysis for Rapid Determination of Mercury in Skincare Products Based on Fluorescence Quenching of Eco-Friendly Synthesized Carbon Dots

Kanokwan Sakunrungrit, Cheewita Suwanchawalit, Kanokwan Charoenkitamorn, Apisake Hongwitayakorn, Kamil Strzelak, and Sumonmarn Chaneam*

Cite This: *ACS Omega* 2023, 8, 7615−7625

Read Online

ACCESS | Metrics & More | Article Recommendations

ABSTRACT: This work reports the analysis of mercury using a spectrofluorometric method combined with a sequential injection analysis (SIA) system. This method is based on the measurement of fluorescence intensity of carbon dots (CDs), which is quenched proportionally after adding mercury ions. Herein, the CDs underwent environmentally friendly synthesis using a microwave-assisted approach that provides intensive and efficient energy and shortens reaction time. After irradiation at 750 W for 5 min in a microwave oven, a dark brown CD solution with a concentration of 2.7 mg mL^{-1} was obtained. The properties of the CDs were characterized by transmission electron microscopy, X-ray diffractometry, X-ray photoelectron spectroscopy, Fourier-transform infrared spectroscopy, and UV−vis spectrometry. We presented for the first time the use of CDs as a specific reagent for the determination of mercury in skincare products with the SIA system to achieve rapid analysis and full automatic control. The as-prepared CD stock solution was diluted 10 times and used as a reagent in the SIA system. Excitation and emission wavelengths at 360 and 452 nm, respectively, were used to construct a calibration curve. Physical parameters affecting the SIA performance were optimized. In addition, the effect of pH and other ions was investigated. Under the optimum conditions, our method showed a linear range from 0.3 to 600 mg L^{-1} with an R^2 of 0.99. The limit of detection was 0.1 mg L^{-1}. Relative standard deviation was 1.53% (n = 12) with a high sample throughput of 20 samples per hour. Finally, the accuracy of our method was validated by comparison using inductively coupled plasma mass spectrometry. Acceptable recoveries were also presented without a significant matrix effect. This method was also the first time that uses the untreated CDs for the determination of mercury(II) in skincare products. Therefore, this method could be an alternative for mercuric toxic control in other sample applications.

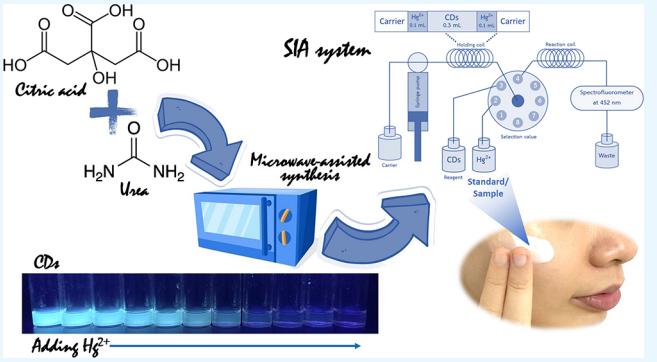

1. INTRODUCTION

At present, there has been increasing concern about the safety of cosmetic and pharmaceutical products used in everyday life. Mercury is a toxic metal that presents intentionally or accidentally in some treatments of skin conditions, particularly whitening products. Mercury can be presented in these products, although it is not listed on the label or on the product information. However, it may accumulate in the skin and exert harmful side effects on the skin and internal organs when used in large quantities for a long period of time. For example, in the case of a woman who uses mercury-containing cream, mercury levels are high in the hair, blood, and urine. The long-term use of mercury-containing lighteners often produces a gray skin color.[1−3] Therefore, many countries, including Thailand, have prohibited the use of mercury in these products not higher than 1 mg L^{-1}.[4] In Thailand, face whitening cream holds a 60% share of the national market for facial lotion, with approximately 2100 million Baht ($70 million).[5] Therefore, increasing public awareness about mercury contamination in skincare products is necessary.

Traditional techniques have been utilized for detecting mercury ions (Hg^{2+}) in skincare and cosmetic products such as titration,[6] neutron activation analysis,[7] and cold vapor atomic absorption spectrometry.[8] Inductively coupled plasma mass spectrometry (ICP-MS) has become a powerful analytical technique for Hg^{2+} analysis.[9,10] However, the instrument is

Received: November 7, 2022
Accepted: February 1, 2023
Published: February 14, 2023

https://doi.org/10.1021/acsomega.2c07175
ACS Omega 2023, 8, 7615−7625

expensive, and it requires highly skilled operators. An alternative for optical sensing systems for the detection of Hg^{2+} can also be based on the fluorescence assay because of its high sensitivity and fast analysis. Many fluorescent probes, including organic molecules, have been developed for fluorescent Hg^{2+} detection in various samples based on the ionophore/fluorophore reagent.[11−14] However, some reagents have difficult and multistep synthesis, a considerable amount of products, and chemical toxicity. In addition, most reagents are insoluble in an aqueous medium, which is an unfavorable condition of the sample preparation medium and of the flow-based system including the sequential injection analysis system (SIA). There are previous works reported using the SIA for determination of Hg^{2+}, for example, SIA with cold vapor atomic absorption spectrometry,[15] SIA with anodic stripping voltammetry,[16] and SIA with spectrophotometry.[17]

Nanoparticles have been used to address the abovementioned problems. Recent advances in nanotechnology have provided new methodologies for Hg^{2+} sensing contaminants.[18,19] For example, colorimetric methods based on surface plasmon resonance of gold nanoparticles have been used for testing Hg^{2+}.[20] However, these gold nanoparticles are unstable, and they require time-consuming modification processes. Among these nanoparticles, carbon-based nanomaterials such as carbon dots (CDs) are increasingly used in various fields, including food, agricultural, industrial, health, and medical purposes, because of their unique physical and chemical properties. CDs have easy synthesis, biocompatibility, and low toxicity.[21] Elemental analysis showed that CDs are composed of C, H, O, and N, depending on the carbon precursors. In general, CDs should be further purified by using centrifugation, dialysis, electrophoresis, or another separation technique to control the size and improve the photoluminescence properties. Some studies use CDs as a specific sensor for heavy metals.[22−27] Most of the CD probes for Hg^{2+} were applied to analyze Hg^{2+} in water samples[28−32] and breast milk.[33] In addition, CDs were investigated as the Hg^{2+} sensor for bioimaging.[34,35]

As described previously, CDs have been applied for Hg^{2+} analysis. However, CDs have never been applied for the assessment of Hg^{2+} in skincare products. Herein, we presented an easy preparation of CDs through a one-step and short-time method under a microwave-assisted approach by using common chemical reagents such as citric acid and urea as initial substances. The resultant CDs exhibited strong blue fluorescence emission in aqueous solution. After adding Hg^{2+} to the untreated CD solution, precipitation and aggregation of Hg-CDs occurred. Simultaneously, fluorescence emission of the solution turned off. Based on this phenomenon, a fluorometric detection was explored and used for quantitative analysis of mercury.

In this work, the feasibility of CDs for Hg^{2+} analysis in a real sample was also demonstrated by employing the SIA system for microliter handling to reduce the sample and reagent as well as achieve the automatic operation. The developed procedure was applied to monitor the Hg^{2+} content in skincare products, particularly whitening cream.

2. EXPERIMENTAL SECTION

2.1. Materials and Instruments. All the experiments were performed in aqueous solution. Citric acid anhydrous 99.5% (Loba Chemie Pvt., Ltd., India) and urea 99.5% (Loba Chemie Pvt., Ltd., India) were used for CD synthesis. The standard solution of 1000 mg/L Hg^{2+} was prepared by dissolving mercury(II) acetate (Sigma-Aldrich, USA) in deionized water and used as a stock solution. The working standard solution of 0.3−600 mg L^{-1} Hg^{2+} was prepared by diluting the stock solution. Acetate buffer (0.10 M) at pH 6 and 7 was prepared from acetic acid (Carlo Erba, Italy) and sodium acetate (Sigma-Aldrich, USA). Phosphate buffer (0.1 M) at pH 6 was prepared from sodium phosphate (Sigma-Aldrich, USA). All of the solutions were prepared in deionized water.

In this work, we aimed to quantitatively analyze Hg^{2+} in skincare products. Different products for skin conditions, particularly whitening cream, were purchased from the online market, local cosmetic shops, and supermarkets in Nakhon Pathom, Thailand. For analysis, the exact weight of 0.10 g of the sample was dissolved in 0.50 mL of 5% (v/v) HNO_3 (Carlo Erba, Italy), and the volume was made to 25 mL in a volumetric flask by 0.1 M acetated buffer at pH 7.0, which was then injected to the SIA system. All samples were analyzed using the proposed flow system and the ICP-MS reference method.

2.2. Microwave-Assisted Synthesis of CDs. The CDs were synthesized by a microwave-assisted method of the previously reported procedure with a slight modification.[36,37] The mixed solution composed of 1.00 g of citric acid and 1.00 g of urea to 10.00 mL of deionized water was irradiated at 750 W for 5 min in a microwave oven (Samsung model MW71B) to give the CD suspension. Finally, the as-synthesized CDs were collected and stored at 4 °C for further characterization and application of Hg^{2+} detection.

Fluorescence quantum yield (QY) was determined by a comparative method.[38−40] Quinine sulfate in 0.1 M H_2SO_4 was used as a standard solution to calculate the QY of synthesized CD samples, which were dissolved in deionized water. All the absorbance values of the solutions at the excitation wavelength were measured with a UV−vis spectrophotometer. Photoluminescence (PL) emission spectra of all the sample solutions were recorded by a PerkinElmer LS-50B luminescence spectrometer at an excitation wavelength of 360 nm. The fluorescence quantum yield of the as-prepared CDs was calculated by comparing the UV−vis absorbance values and the integrated fluorescence intensities (λ_{ex} = 360 nm) of the CDs with those of quinine sulfate solution. The absorbance values of all solutions were maintained under 0.05 to minimize self-absorption. The fluorescence quantum yield of obtained CDs was calculated using the following equation:

$$\varphi_u = \varphi_s \frac{F_u A_s \eta_u^2}{F_s A_u \eta_s^2}$$

where φ is the quantum yield, A stands for the optical density, F represents the integrated emission intensity, and η is the refractive index of the solvent. "s" and "u" correspond to the standard and the sample, respectively.

2.3. Microwave Digestion and ICP-MS for Method Validation. For sample preparation, microwave digestion was used. The exact weight of 0.20 g of each sample was transferred into a microwave vessel. Then, 9.00 mL of nitric acid (conc. 65%, w/w) and hydrogen peroxide (conc. 30% w/w) was added into the microwave vessel as digestion reagents. Finally, under microwave digestion around 50 min, the sample solution was transferred into a volumetric flask, and the volume was made up to 100 mL with deionized water. Afterward, the prepared sample solutions were analyzed by ICP-MS. ICP-MS (7900 ICP-MS, Agilent, USA), with a detection limit of mercury of 0.001 mg

https://doi.org/10.1021/acsomega.2c07175
ACS Omega 2023, 8, 7615−7625

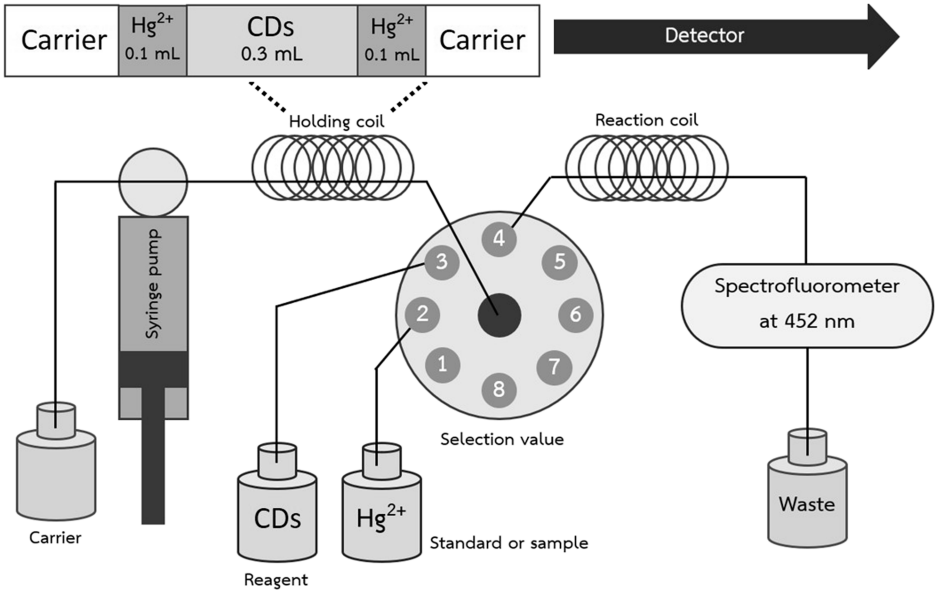

Figure 1. Schematic diagram of the SIA system for the determination of mercury.

L^{-1}, was used as the standard method to validate mercury analysis.

2.4. Characterizations. The properties of the as-prepared CDs before and after reacting with Hg^{2+} were characterized extensively. The structures and morphologies were examined using X-ray diffractometry (XRD; Aris, PANalytical, UK), X-ray photoelectron spectroscopy (XPS) (Kratos Axis Ultra spectrometer, Manchester, UK, with a monochromic Al Kα source at 1486.7 eV), and transmission electron microscopy (TEM) (FE-TEM/STEM-EDS, Thermo Scientific Talos F200X STEM, USA). Fourier-transform infrared spectra of standard mercury-(II) acetate, dried CDs, and dried Hg-CDs were recorded on Frontier, PerkinElmer, USA. UV−visible absorption spectra were recorded on Cary 60, Agilent, USA, and fluorescence spectra were recorded using a spectrofluorometer (LS 55, PerkinElmer, USA).

2.5. Sequential Injection Procedure. The SIA with a syringe pump (Cavro XLP 6000, Switzerland) and a selection valve (Cavro Smart Valve, Switzerland) was operated (Figure 1). A 5 mL zero-dead-volume syringe was fitted with a holding coil. The programmable pump and valve were automatically controlled, via an RS-232 communication port, using the program developed in C# language running under an MS-Windows environment. The graphical user interface of the program practically guided users to input parameters and steps of the procedure as necessary. The amount of Hg^{2+} in skincare products was determined using an SIA coupled spectrofluorometer. As shown in Table 1, the common sequential injection procedure has five steps for one cycle. First, a 3000 μL carrier was aspirated into the system at a flow rate of 10 mL min^{-1}. Next, two 100 μL segments of standard or sample (port 2) partition with a 300 μL segment of the diluted CD solution (port 3) were sequentially aspirated into a holding coil, namely, sandwich pattern, at a flow rate of 10 mL min^{-1}. Then, zone stacking was sent to a reaction coil (PTFE, 0.75 mm, 100 cm) and continuously propelled to the detection cell through port 4 at a flow rate of 2.5 mL min^{-1} with no need of any cleaning step. The fluorescence intensity was recorded at an excitation wavelength and emission wavelength of 360 and 452 nm, respectively. A decreased signal (compared with the blank sample) was observed because the fluorescence of the CDs was quenched by Hg^{2+} in the sample.

Table 1. SIA Procedure Operated in This Work

step	flow rate (mL min^{-1})	volume (μL)	flow direction	event
1	10	3000	reverse	carrier aspirated
2	10	100	reverse	standard/sample zone segment 1 aspirated
3	10	300	reverse	reagent zone aspirated
4	10	100	reverse	standard/sample zone segment 2 aspirated
5	2.5	3500	forward	zones sent to the spectrofluorometer

3. RESULTS AND DISCUSSION

3.1. Concentration and Size of CDs. The CDs were synthesized by a microwave-assisted method as described above. A hundred microliters of the as-prepared CD solution was pipetted onto a glass slide and was evaporated at 80 °C for 24 h. Finally, the concentration of the synthesized CDs was found to be 2.7 mg mL^{-1}. The fluorescence quantum yield of the CDs was calculated to be about 0.16%. This result might be due to the effect of low energy transfer of large untreated CDs. However, this QY value is sufficient for our application. To use the CDs as a reagent in the SIA system, the optimal concentration of the CD solution was investigated by dilution to 0.54, 0.27, and 0.14 mg mL^{-1} and the concentration of 0.27 mg L^{-1} showed the best sensitivity. Therefore, the as-prepared stock CD solution was diluted 10 times in deionized water. The clear diluted CD solution was used as a reagent for Hg^{2+} analysis with the SIA. The stability of the CDs was also investigated by measuring the fluorescence intensity and sensitivity of the flow system for Hg^{2+} determination. The results revealed that the sensitivity of our system was stable up to 3 months after preparation. Precision of synthesis was considered by measuring the emission intensity at 452 nm of the 10 times dilution of the as-prepared CDs obtained from each batch. Therefore, inter-batch precision of the synthesis of CDs was reported as 2.9%RSD (n = 3).

https://doi.org/10.1021/acsomega.2c07175
ACS Omega 2023, 8, 7615−7625

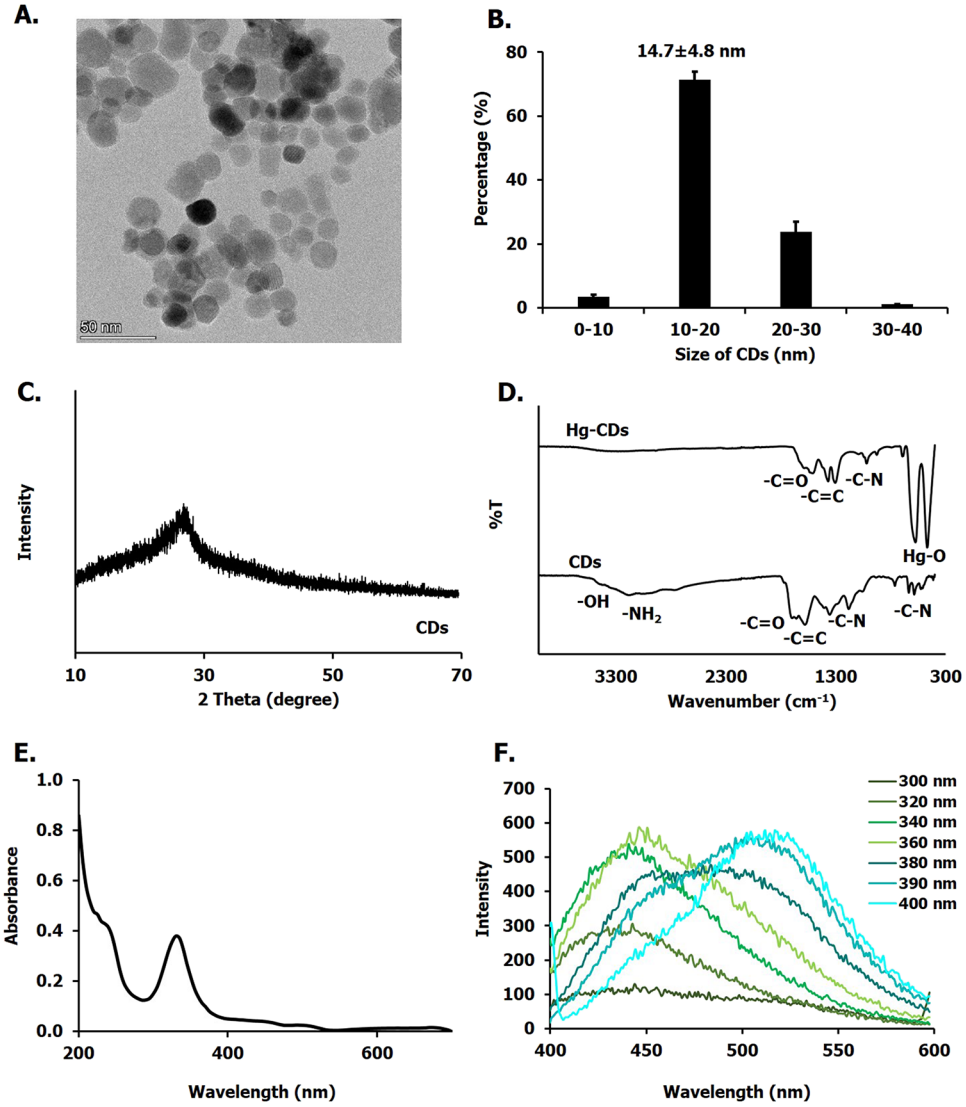

Figure 2. Typical TEM image of as-prepared CDs (A) and CDs' size distribution (B). XRD pattern of the as-prepared CDs (C). FT-IR spectra of the synthesized CDs and Hg-CDs (D). The UV−vis spectrum of the CD solution shows absorption at approximately 220−340 nm (E). Photoluminescence emission spectra of the CDs in aqueous solutions at different excitation wavelengths (300−400 nm) (F).

3.2. Characterization of CDs. In this paper, the CDs were synthesized using a microwave-assisted method. TEM was used to characterize the morphology of the untreated CDs. The TEM image (Figure 2A) shows spherical nanoparticles with consistent dispersion. In this work, about 71% of the size distribution is in the range of 10−20 nm (Figure 2B). After analyzing random particles, the CD mean size was 14.7 ± 4.8 nm. A small number of particles are relatively of bigger size because of the agglomeration of smaller particles. Figure 2C shows the XRD patterns of the CDs obtained in the range from 10 to 70°. The XRD pattern shows that the CDs have a broad diffraction peak at 27.2°, which indexes to the (002) plane of graphitic carbon.[41,42] This peak reveals the predominately amorphous structure of the as-prepared CDs.

The surface functional groups of CDs were characterized by FT-IR (Figure 2D). A broad peak of approximately 3420 cm^{-1} was indicative of OH stretching. Absorption bands at 3177 cm^{-1} were attributed to NH_2. These functional groups typically existed on the surface of CDs.[38] The characteristic peaks of the C═O stretching vibration, which are a typical observation for CDs, are shown at 1701 and 1661 cm^{-1}. The 1576 and 1350 cm^{-1} peaks were attributed to the stretching vibrations of C═C and C−N, respectively.[43,44] The FT-IR spectrum of dried Hg-CDs was also evaluated. Two peaks at approximately 400−600 cm^{-1} were found dominant. Based on our reviews in previous works, the characteristic peaks at 576 and 468 cm^{-1} were defined as Hg−O in vibrational mode, which confirms the formation of Hg−O on the surface of Hg-CDs.[45] Notably, the peaks of C═O and broad peaks of −OH and $-NH_2$ were shifted, and their intensities were reduced. The UV−vis spectrum of the CD solution (Figure 2E) shows main absorption bands at approximately 220, 260, and 340 nm, which correspond to the carbon−carbon double bond's $\pi \rightarrow \pi^*$ and aromatic ring's $\pi \rightarrow \pi^*$ transitions. The absorption peak at 340 nm in the UV−vis absorption spectra of the synthesized CDs confirmed that the presence of the C═C functional group of the graphitic structure occurs during the carbonization process.[46,47] As shown in Figure 2F, when the CDs were excited at 360 nm, strong fluorescence emission at 452 nm was observed. The maximum fluorescence peak shifted from 420 to 530 nm with a change of excitation wavelength from 300 to 400 nm, respectively.

https://doi.org/10.1021/acsomega.2c07175
ACS Omega 2023, 8, 7615−7625

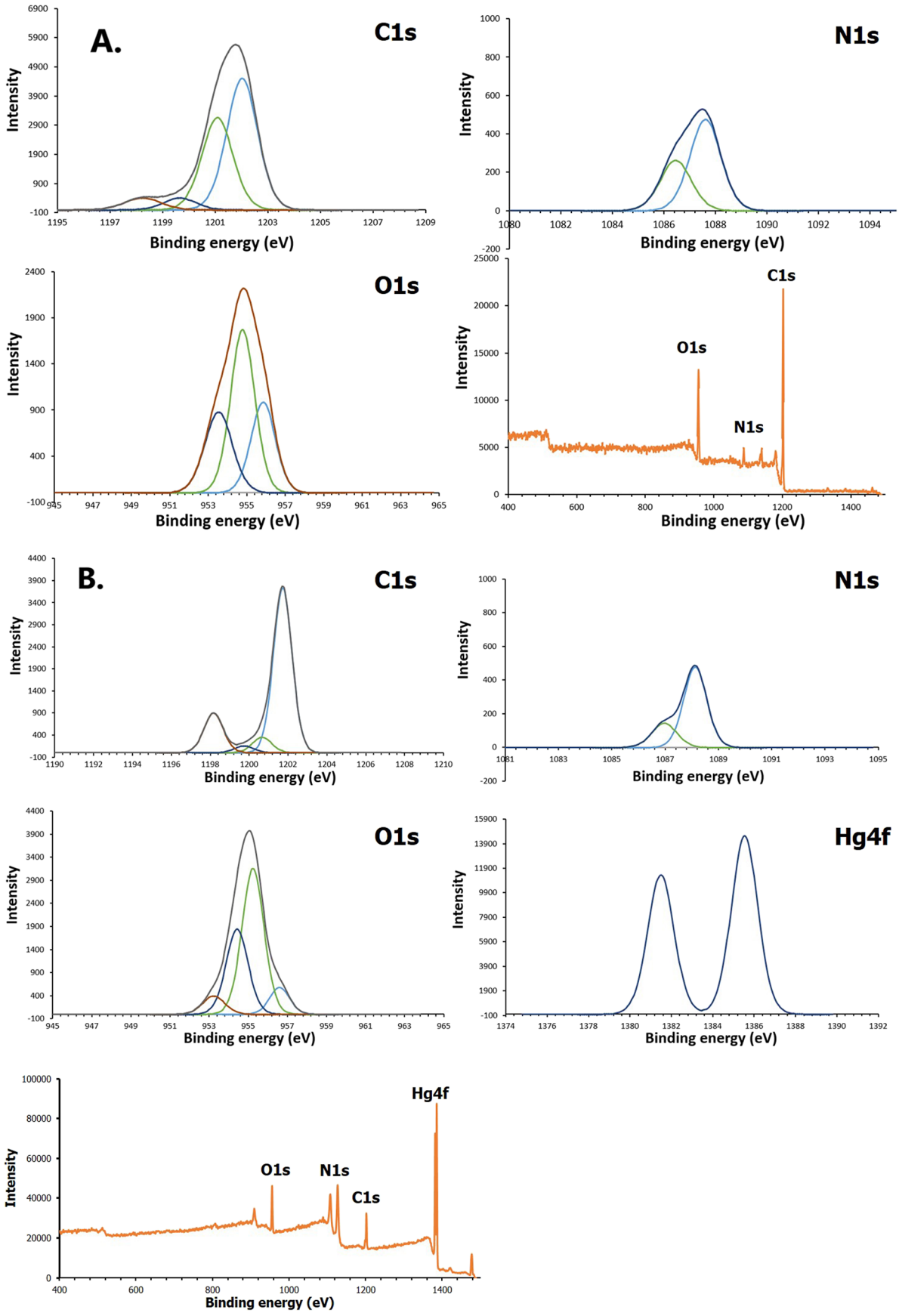

Figure 3. XPS spectra of the CD (A) and Hg-CD products (B) obtained.

https://doi.org/10.1021/acsomega.2c07175
ACS Omega 2023, 8, 7615−7625

Furthermore, elemental compositions of CDs and Hg-CDs were also investigated by the XPS technique.[37,47,48] Figure 3 presents the high-resolution XPS spectra of C (1s), N (1s), O (1s), and Hg (4f) of CDs and Hg-CDs. The XPS survey scan spectrum of the CDs (Figure 3A) revealed three apparent binding peaks corresponding to the O (1s), N (1s), and C (1s). The deconvolution spectrum of C (1s) showed four peaks at 284.64, 285.59, 287.05, and 288.44 eV, which can be attributed to C═C (sp^2), C−N, C−OH/C−O−C, and C═O groups, respectively.[49] The high-resolution N (1s) spectrum (Figure 3A) was deconvoluted into two peaks at 399.07 and 400.22 eV, corresponding to C−NH_2 and O═N—C functional groups, respectively. The O (1s) spectrum (Figure 3A) was deconvoluted to three peaks at 530.84, 531.91, and 533.14 eV, indicating the presence of −C−O/−N−O, —C═O, and C−O−C functional groups, respectively.[50,51] The XPS results confirmed that there are many functional groups (−NH_2, −COOH, and −OH) on the surface of CDs corresponding with FT-IR results. The XPS spectra of the Hg-CDs (Figure 3B) are composed of O, N, C, and Hg elements. The C (1s) spectrum could be deconvoluted into four peaks at 284.94, 286.03, 286.96, and 288.52 eV, corresponding to the C═C (sp^2), C−N, O—C═O, and C═O groups, respectively.[49] The N (1s) spectrum reveals the presence of the amine group (C−NH_2 (398.56 eV) and O═N—C (399.74 eV)). The O (1s) spectrum was deconvoluted to four peaks at 530.09, 531.47, 532.28, and 533.47 eV, suggesting the presence of −C−O/−N−O, —C═O, C−OH, and C−O−C groups, respectively.[48,50,51] For Hg, the (4f) spectrum found two peaks of 4f5/2 and 4f7/2 at 105.18 and 101.13 eV, respectively.[52] The results showed that mercury was adsorbed on CDs via oxygen-containing functional groups and amine group in the adsorption of mercury ions.[48,52]

3.3. Detection of Mercury Ions Using the Batch Method. Fluorescence quenching of CDs was achieved by hand mixing the aqueous solutions of CDs and Hg^{2+}. At first, Figure 4 presents images of the untreated CDs and products after reacting with Hg^{2+} under visible (Figure 4A) and UV light (Figure 4B). The bright blue photoluminescence is strong and easily seen with the naked eyes. In addition, 100 μL of the diluted CDs was added to 3.00 mL of deionized water in a quartz cuvette, and the fluorescence intensity of CDs was recorded as blank. Then, the standard solution of 0−100 μL of 1000 mg L^{-1} Hg^{2+} was added into 10 μL of solution increment each time. Afterward, the solution was mixed by shaking the cuvette. After Hg^{2+} was introduced into the CD solution, Hg-CD aggregation was induced; thus, fluorescence intensity of the CDs disappears soon. The aggregation of CDs is enforced upon the addition of the mercury ion. Consequently, the color of solution turns from pale yellow to colorless. However, UV−visible absorption of CDs and CDs after adding Hg^{2+} solution is less sensitive, and it could not be applied to real samples. Therefore, photoluminescence was used by measuring the maximum emission peak at 452 nm with an excitation at 365 nm. As shown in Figure 5A,B, the fluorescence intensity decreased gradually with the increase in Hg^{2+} concentration. The formation of non-luminescent Hg-CD aggregation might lead to quenching of fluorescence intensity. A linear calibration curve (Figure 5C) was obtained, and it shows that the untreated CDs could be utilized for quantitative analysis of Hg^{2+}. Based on the above results, high selectivity toward Hg^{2+} in aqueous solution could be probably a coordinative interaction with Hg^{2+} and the carboxyl and hydroxyl groups on the surface of CDs. The photoluminescence intensity decreases with the increasing concentrations of Hg^{2+}. The photoluminescence quenching of CDs was caused by Hg^{2+}chelation between surface functional groups of CDs and Hg^{2+} via charge transfer, leading to the fluorescence quenching of the CDs.[53−56]

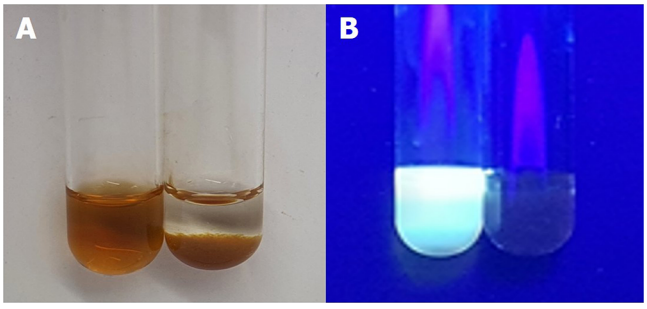

Figure 4. Photographs under visible (A; daylight lamp) and UV light (B; λ_{ex} = 365 nm). (The concentration of CDs is 0.27 mg mL^{-1}, and the concentration of Hg^{2+} is 60 mmol L^{-1}). All photos were taken by S.C.

A dependence of the CD fluorescence intensity on the pH value was reported. Similar to previous works,[21] we found that the intensity decreased when the pH value of the CD solution was lower than 5. The fluorescence intensity of Hg-CDs is also pH-dependent (Figure 5D). At the acidic medium, low quenching efficiency was observed, which results from the dissociation of the Hg-CD compound caused by the protonation of surface-binding carboxyls. With the increase in pH, the deprotonation of the carboxylic groups in the CDs occurs. This phenomenon may strengthen the covalent bond between Hg^{2+} and CDs, which leads to higher quenching efficiency and lower fluorescence intensity.[37] At the high basic medium, the precipitate of mercury hydroxide might occur and reduce the Hg-CD compound. From the results, pH 7.0 was used. Various types of medium solutions at pH 7 were further studied, which are DI water, acetate buffer, and phosphate buffer, and the results show that acetate buffer at pH 7 gives the best sensitivity.

3.4. Optimization of Physical Parameters Affecting the SIA Performance. The experiment is shown in Figure 1. The working standard solution of 0.3−600 mg L^{-1} Hg^{2+} was used to optimize the physical parameters. First, the volumes of the sample and reagent were optimized to reduce their amount (Figure 6A,B). Notably, the solution volume needed for the proposed SIA method can be reduced to the microliter level. We found that 200 μL of the sample (divided in two aliquots of 100 μL intercalated with the reagent aliquot) was sufficient to cover the analysis range with a satisfactory signal, and the CD reagent solution at 300 μL was selected for all further experiments. Next, the flow rate sent to the spectrofluorometer, which has a significant effect on the measured signal, was studied. In this experiment, the flow rate varied from 2.5, 5, 10, and 15 mL min^{-1}. As shown in Figure 6C, the sensitivity decreased when the flow rate was increased. In accordance with the sensitivity, we selected 2.5 mL min^{-1} as the optimal flow rate. In addition, we observed that even if a flow rate higher than 10 mL min^{-1} was used, sample throughput was not significantly improved, but a large noise was observed. At a 2.5 mL min^{-1} flow rate, we obtained a satisfactorily high throughput of 20 sample h^{-1}.

3.5. Effect of Other Metal Ions. Figure 7 shows the results of the effect of coexisting metal ions. First, batch experiments were performed by evaluating the fluorescence intensity under UV light. A hundred microliters of diluted CDs was added to a medium of 3.00 mL of DI water in a vial, and then, 80 μL of 100

https://doi.org/10.1021/acsomega.2c07175
ACS Omega 2023, 8, 7615−7625

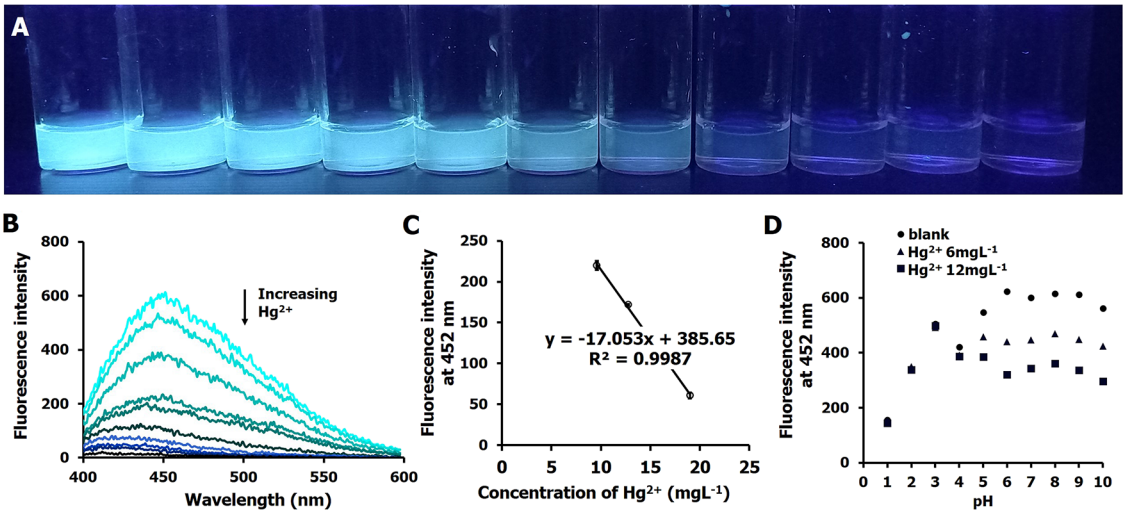

Figure 5. Corresponding fluorescence images under a 365 nm UV lamp (A) taken by S.C. and fluorescence emission spectra of a mixture of CDs with the addition of Hg^{2+} (B). Calibration curve plot of fluorescence intensity at 452 nm at various concentrations of Hg^{2+} (C). Effect of pH on the fluorescence intensity (D).

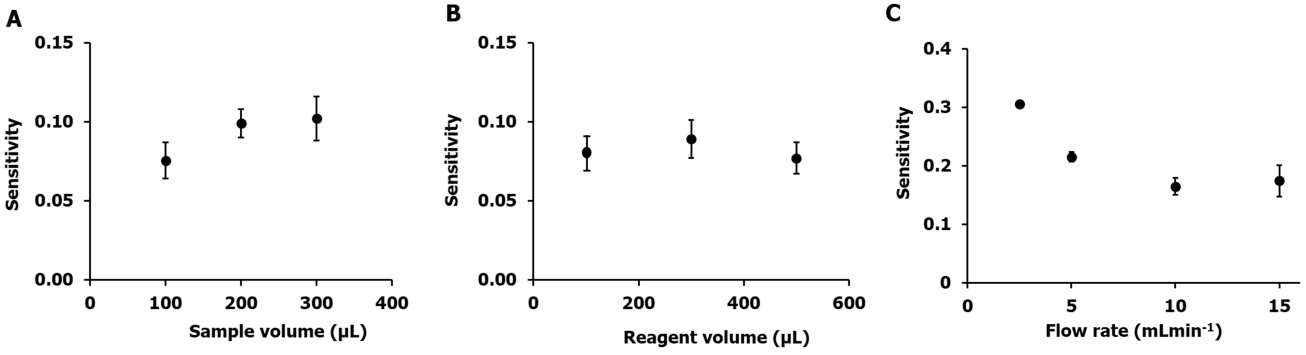

Figure 6. Sensitivity of calibration curves obtained from physical parameter studies: sample volume (A), reagent volume (B), and flow rate to detector (C). The optimized conditions are as follows: a flow rate of 2.5 mL min^{-1}, volumes of the sample and reagent of 0.2 and 0.3 mL, respectively, and no waiting time.

mg L^{-1} metal ion solution was added (Figure 7A). The fluorescence intensity was recorded with an emission wavelength of 452 nm and excitation wavelength of 360 nm (Figure 7B). The effect of metal ions on Hg^{2+} detection was also investigated by injecting 200 μL of 100 mg L^{-1} for each metal ion solution into the SIA system, and the signal profile and bar graph are shown in Figure 7C and Figure 7D, respectively, which were consistent with the data obtained from the batch experiment (Figure 7A,B). Notably, interferences were not observed from Cd^{2+}, Ba^{2+}, Ni^{2+}, Ca^{2+}, Na^{+}, K^{+}, and Zn^{2+}. Pb^{2+} and Mn^{2+} had a slight effect on the fluorescence intensity, which could be negligible. This result may be due to the stability constants between the Hg^{2+} and carboxylic group, which are higher than other metal ions leading to the formation of a Hg−O non-fluorescent metal adduct.[52] In the case of Fe^{2+} and Cu^{2+}, less fluorescence intensity might result from metal hydroxide precipitation. Quenching of CDs by Fe^{2+} and Cu^{2+} was also found in previous works.[33] In addition, 2 and 20 mg L^{-1} Fe^{2+} and Cu^{2+} were tested by injecting to the SIA system. The results showed that our method can tolerate the presence of Fe^{2+} and Cu^{2+} at the tested levels. However, these ions are rarely found in the tested skincare products.

3.6. Analytical Features. Figure 8A illustrates the signal profile obtained from the SIA system with various concentrations of Hg^{2+} and calibration curve obtained from the signal profile for the determination of Hg^{2+} in samples (Figure 8B). The horizontal axis is the concentration of Hg^{2+} in mg L^{-1}, and the vertical axis is the difference between fluorescence intensity of blank (I_0) and fluorescence intensity of the sample (I_s). The linear equation of 0.3−10 mg L^{-1} is $y = (0.846 \pm 0.040)x + (4.243 \pm 0.192)$ with $R^2 = 0.991$ and of 10−600 mg L^{-1} is $y = (0.129 \pm 0.006)x + (12.123 \pm 2.119)$ with $R^2 = 0.991$. The results showed that good precision with standard deviation and relative standard deviation for Hg^{2+} are 2.30 and 1.53%, respectively ($n = 12$). This method has short-time analysis with a sample throughput of 20 samples per hour. The limit of detection, that is, the ratio of 3 times the standard deviation of the background and the slope of the linear function (3 s/S), was calculated to be as low as 0.1 mg L^{-1}, which is lower than the permitted limit of mercury in skincare products in Thailand.[4] In addition, the U.S. FDA regulations also say about prohibited and restricted ingredients in cosmetics, which are limited to 65 mg Hg L^{-1} for eye area products and 1 mg Hg L^{-1} for all other cosmetics. Its presence is unavoidable under conditions of good manufacturing practice (21 CFR 700.13).[57] It should be noted that the analytical features of our proposed method are sufficient for determination of mercury in skincare products. Table 2 shows the figures of merit for some of the previously reported

https://doi.org/10.1021/acsomega.2c07175
ACS Omega 2023, 8, 7615−7625

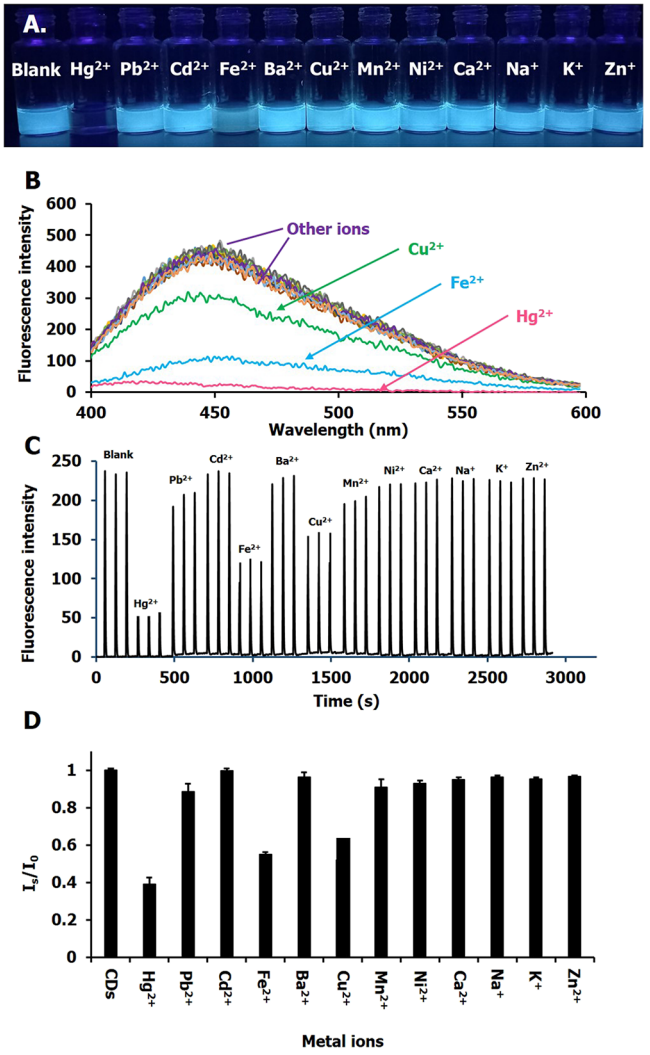

Figure 7. Photograph of fluorescence change under UV light (A) taken by S.C. and emission spectra (B) of diluted CDs in acetate buffer pH 7.0 solution upon the addition of various metal ions, including Hg^{2+}, Pb^{2+}, Cd^{2+}, Fe^{2+}, Ba^{2+}, Cu^{2+}, Mn^{2+}, Ni^{2+}, Ca^{2+}, Na^{+}, K^{+}, and Zn^{2+}. SIA experiments with the same set of foreign metal ions used acetate buffer pH 7.0 solution as the carrier (C, D).

methods and our method. This method has easy synthesis, and it uses untreated CDs without the need of any modifications. In addition, the measuring procedure is controlled automatically by a computer.

3.7. Sample Analysis and Method Validation. The applicability of the proposed method was evaluated by analyzing skincare products (sampled from Nakhon Pathom, Thailand) as real samples. First, the original samples were analyzed using the proposed SIA method and the reference ICP-MS. Notably, no Hg^{2+} was observed in all samples. Although Hg^{2+} was not found in the tested skincare samples, the result agreed well with that obtained from ICP-MS (with a detection limit of Hg^{2+} as low as 0.001 mg L^{-1}). The matrix effect of skincare was investigated by using spiked samples of 1 mg L^{-1} Hg^{2+}. For SIA, the sample solutions were directly injected into the system. For ICP-MS, a dilution factor of 100 was applied and then calculated backwards. Recoveries of each method are calculated and reported in Table 3. By comparison of %recoveries obtained from the SIA and ICP-MS, although %relative errors of some samples were carried out at ±5%,[58] their %recoveries are acceptable according to the AOAC method performance requirements for heavy metal analysis, which are in the range of 80−115.[59] The accuracy of our method was further evaluated by triplicate measurements of reference solution Hg^{2+} (Agilent part number 8500-6940-HG), certified as 1.0 mg L^{-1}.[60] The analysis of this sample using the proposed system showed that the fluorescence intensity measurement Hg^{2+} was 1.01 ± 0.02 mg L^{-1}. This result indicates the potential application of this procedure in monitoring hazardous Hg^{2+}.

4. CONCLUSIONS

Photoluminescent CDs have shown great application in potential health and medical fields. Here, we have utilized the microwave-assisted synthesis of untreated CDs as a specific reagent in the SIA system for the detection of heavy metal ions, which is mercury. In this work, although our CDs have a size of 14.7 ± 4.8 nm in average, the CDs exhibited good optical properties investigated corresponding to the "dots".[61] The CDs showed potential as mercury ion sensors with a detection limit of 0.1 mg L^{-1}. There are several advantages, such as a wider linear range and easy synthesis without the need for later purification and modification steps. No significant difference was observed between the results from our method and the results from ICP-

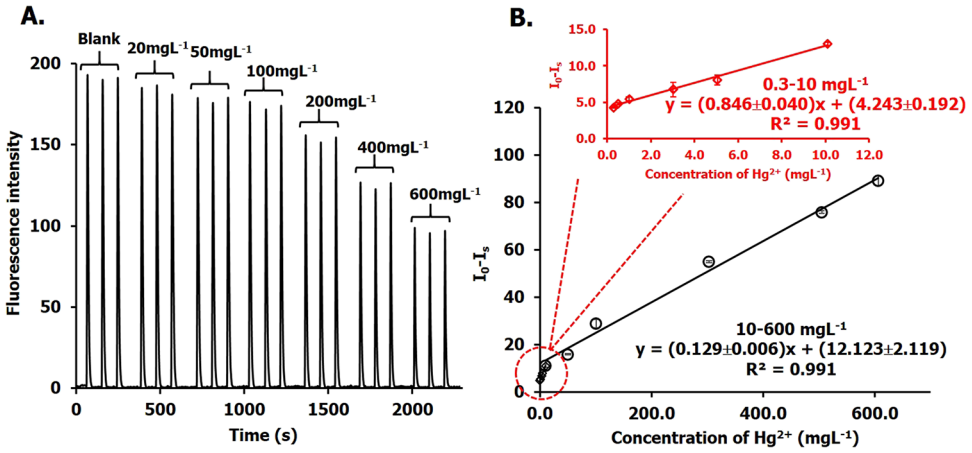

Figure 8. Signal profile (A) and calibration curve (B) obtained from the proposed SIA operated under the optimum conditions. Error bars are derived from three injections.

https://doi.org/10.1021/acsomega.2c07175
ACS Omega 2023, 8, 7615−7625

Table 2. Figures of Merit for Some of the Previous Reports Utilizing CDs as a Reagent for Mercury Analysis

Sample	CD precursor	Synthesis procedure	Linear range	Precision	LOD	Automatics	Reference
Lake water	Flour	Microwave-assisted	0.0005–0.01 μmol L^{-1}	Not reported	0.5 nmol L^{-1}	×	37
Tap water	Urea and ethylenediamine tetraacetic acid (EDTA)	One-step pyrolysis	0.001–8 μmol L^{-1}	Not reported	6.2 nmol L^{-1}	×	51
Tap water	Citric acid and triethylamine	Hydrothermal	0.05–7 μmol L^{-1}	Not reported	2.8 nmol L^{-1}	×	52
Breast milk	Citric acid and melamine	Solid thermal method	2–14 μmol L^{-1}	%RSD < 6	0.44 μmol L^{-1}	×	33
Tap water and packed water	Citrus lemon juice and ethylenediamine	Hydrothermal	0.001–1 μmol L^{-1}	%RSD 1.32	5.3 nmol L^{-1}	×	34
Tap water	Citric acid and 2,2-dimethyl-1,3-propanediamine	Microwave-assisted pyrolysis	0–4.2 μmol L^{-1}	%RSD < 2	7.63 nmol L^{-1}	×	28
Tap water and lake water	Eggshell membrane	Hydrothermal	10–100 μmol L^{-1}	Not reported	2.6 μmol L^{-1}	×	29
skincare products	Acetic and urea	Microwave-assisted (untreated)	1.5–2991 μmol L^{-1} (0.3–600 mg L^{-1})	%RSD 1.53	0.5 μmol L^{-1} (0.1 mg L^{-1})	✓ 20 sample h^{-1}	This work

Table 3. Analysis Results of the Detection of Hg^{2+} in Real Samples from Triplicate Analysis Comparison with ICP-MS and Recovery Results of the Actual Samples (ND = Not Detectable)

	Hg^{2+} (mg L^{-1})				
	standard method (ICP-MS)	proposed method			
sample[a]	original	%recovery[b,c]	original	%recovery[b,c]	%relative error[d]
1	ND	101.10	ND	87.1 ± 2.4	−13.8
2	ND	100.83	ND	82.4 ± 3.9	−18.3
3	ND	90.77	ND	86.6 ± 1.0	−4.6
4	ND	98.66	ND	81.8 ± 6.6	−17.1
5	ND	109.56	ND	114.0 ± 5.7	4.05
6	ND	105.42	ND	104.2 ± 3.8	−1.16
7	ND	93.94	ND	85.2 ± 2.7	−9.30
8	ND	100.60	ND	88.7 ± 2.9	−11.8
9	ND	105.94	ND	92.6 ± 3.4	−12.6

[a]Sample nos. 1−5 were the whitening face serum, no. 6 was the soothing gel, and nos. 7−9 were serum lotion. [b]%recovery = [(concentration of spiked standard mercury solution − concentration of the sample)/concentration of standard mercury solution] × 100. [c]The concentration of spiked standard mercury solution for ICP-MS and the proposed method is 1 mg L^{-1}. [d]%relative error = [(%$recovery_{proposed\ method}$ − %$recovery_{std\ method}$)/%$recovery_{std\ method}$] × 100.

MS with an acceptable percentage recovery of 81.8−114. This method provides less recovery; however, the feature of cost-effectiveness and convenience is better compared to the standard ICP-MS. The SIA application based on CDs was developed for the first time, providing a simple, automatic, rapid, and low-cost analysis platform for the detection of mercury ions in skincare products and heavy metal ion contamination. Our method is environmentally friendly because the detection does not rely on any toxic chemical reaction. Therefore, this system has received considerable attention from scientists working with quality control or working for agencies of safety and inspection service. Furthermore, the SIA system could be further developed as a portable device for on-site analysis.

AUTHOR INFORMATION

Corresponding Author

Sumonmarn Chaneam − *Department of Chemistry, Faculty of Science, Silpakorn University, Nakhon Pathom 73000, Thailand; Flow Innovation Research for Science and Technology Laboratories (FIRST Labs), Bangkok 10400, Thailand;* orcid.org/0000-0002-2753-9642; Phone: +66 3 4255797; Email: chaneam_s@su.ac.th; Fax: +66 3 4271356

Authors

Kanokwan Sakunrungrit − *Department of Chemistry, Faculty of Science, Silpakorn University, Nakhon Pathom 73000, Thailand*

Cheewita Suwanchawalit − *Department of Chemistry, Faculty of Science, Silpakorn University, Nakhon Pathom 73000, Thailand*

Kanokwan Charoenkitamorn − *Department of Chemistry, Faculty of Science, Silpakorn University, Nakhon Pathom 73000, Thailand;* orcid.org/0000-0003-4166-8181

https://doi.org/10.1021/acsomega.2c07175
ACS Omega 2023, 8, 7615−7625

Apisake Hongwitayakorn − *Department of Computing, Faculty of Science, Silpakorn University, Nakhon Pathom 73000, Thailand*

Kamil Strzelak − *University of Warsaw, Faculty of Chemistry, 02-093 Warsaw, Poland*

Complete contact information is available at: https://pubs.acs.org/10.1021/acsomega.2c07175

Notes

The authors declare no competing financial interest.

■ ACKNOWLEDGMENTS

Financial support from the Reinventing University System Program by the Ministry of Higher Education, Science, Research, and Innovation is gratefully acknowledged (fiscal year 2021). The authors wish to express their gratitude to the Faculty of Science, Silpakorn University, for the support of this work.

■ REFERENCES

(1) Bourgeois, M.; Dooms-Goossens, A.; Knockaert, D.; Sprengers, D.; Van Boven, M.; Van Tittelboom, T. Mercury intoxication after topical appilcation of a metallic mercury ointment. *Dermatologica* **2004**, *172*, 48−51.

(2) Dyall-Smith, D. J.; Scurry, J. P. Mercury pigmentation and high mercury levels from the use of a cosmetic cream. *Med. J. Aust.* **1990**, *153*, 409−415.

(3) Chan, T. Y. K. Inorganic mercury poisoning associated with skin-lightening cosmetic products. *Clin. Toxicol.* **2011**, *49*, 886−891.

(4) Ministry of Public Health, Ed., *List of Prohibited in Cosmetic Production.*; Ministry of Public Health: Bangkok: 2559.

(5) EARTH, E. A. a. R. T. *Study of mercury contamination in face whitening products in Thailand*; EARTH, E. A. a. R. T.: Thailand, 2021. DOI: https://ipen.org/sites/default/files/documents/EARTH%20Hg%20in%20Whitening%20-%20Report.pdf.

(6) Gaál, F. F.; Abramović, B. F. Determination of mercury content of some pharmaceutical products by catalytic titration. *Microchim. Acta* **1972**, *1*, 465−472.

(7) Margosis, M.; Tanner, J. T. Determination of mercury in pharmaceutical products by neutron activation analysis. *J. Pharm. Sci.* **1972**, *61*, 936−938.

(8) Mallkuci, I.; Lazo, P. MERCURY DETERMINATION IN DRUG AND COSMETIC PRODUCTS. *Int. J. of Curr. Res.* **2014**, *6*, 8077−8082.

(9) Passariello, B.; Barbaro, M.; Quaresima, S.; Casciello, A.; Marabini, A. Determination of mercury by Inductively Coupled Plasma-Mass Spectrometry. *Microchem. J.* **1996**, *54*, 348−354.

(10) Allibone, J.; Fatemian, E.; Walker, P. J. Determination of mercury in potable water by ICP-MS using gold as a stabilising agent. *J. Anal. At. Spectrom.* **1999**, *14*, 235−239.

(11) Kraithong, S.; Sangsuwan, R.; Worawannotai, N.; Sirirak, J.; Charoenpanich, A.; Thamyongkit, P.; Wanichachewa, N. Triple detection modes for Hg^{2+} sensing based on a NBD-fluorescent and colorimetric sensor and its potential in cell imaging. *New J. Chem.* **2018**, *42*, 12412−12420.

(12) Petdum, A.; Panchan, W.; Sirirak, J.; Promarak, V.; Sooksimuang, T.; Wanichacheva, N. Colorimetric and fluorescent sensing of a new FRET system via [5]helicene and rhodamine 6G for Hg^{2+} detection. *New J. Chem.* **2018**, *42*, 1396−1402.

(13) Rasheed, T.; Nabeel, F.; Li, C.; Bilal, M. Rhodamine-assisted fluorescent strategy for the sensitive and selective in-field mapping of environmental pollutant Hg(II) with potential bioimaging. *J. Lumin.* **2019**, *208*, 519−526.

(14) Kaewnok, N.; Sirirak, J.; Jungsuttiwong, S.; Wongnongwa, Y.; Kamkaew, A.; Petdum, A.; Panchan, W.; Sahasithiwat, S.; Sooksimuang, T.; Charoenpanich, A.; Wanichacheva, N. Detection of hazardous mercury ion using [5]helicene-based fluorescence probe with "Turn ON" sensing response for practical applications. *J. Hazard. Mater.* **2021**, *418*, 126242.

(15) Bauzá De Mirabó, F. M.; Thomas, A. C.; Rubí, E.; Forteza, E.; Cerdá, V. Sequential injection analysis system for determination of mercury by cold-vapor atomic absorption spectroscopy. *Anal. Chim. Acta* **1997**, *355*, 203−210.

(16) Punrat, E.; Chuanuwatanakul, S.; Kaneta, T.; Motomizu, S.; Chailapakul, O. Method development for the determination of mercury(II) by sequential injection/anodic stripping voltammetry using an in situ gold-film screen-printed carbon electrode. *J. Electroanal. Chem.* **2014**, *727*, 78−83.

(17) Rattanakit, P.; Prasertboonyai, K.; Liawruangrath, S. Development of sequential injection spectrophotometric method for determination of mercury (II) using pyrogallol red. *Int. J. Environ. Anal. Chem.* **2016**, *96*, 1415−1429.

(18) Du, J.; Zhu, B.; Peng, X.; Chen, X. Optical reading of contaminants in aqueous media based on gold nanoparticles. *Small* **2014**, *10*, 3461−3479.

(19) Zangeneh Kamali, K.; Pandikumar, A.; Jayabal, S.; Ramaraj, R.; Lim, H. N.; Ong, B. H.; Bien, C. S. D.; Kee, Y. Y.; Huang, N. M. Amalgamation based optical and colorimetric sensing of mercury(II) ions with silver@graphene oxide nanocomposite materials. *Microchim. Acta* **2016**, *183*, 369−377.

(20) Lee, J.-S.; Han, M. S.; Mirkin, C. A. Colorimetric Detection of Mercuric Ion (Hg^{2+}) in Aqueous Media using DNA-Functionalized Gold Nanoparticles. *Am. Ethnol.* **2007**, *119*, 4171−4174.

(21) Baker, S. N.; Baker, G. A. Luminescent carbon nanodots: emergent nanolights. *Angew. Chem., Int. Ed.* **2010**, *49*, 6726−6744.

(22) Berlina, A. N.; Zherdev, A. V.; Dzantiev, B. B. Progress in rapid optical assays for heavy metal ions based on the use of nanoparticles and receptor molecules. *Microchim. Acta* **2019**, *186*, 172.

(23) Yoo, D.; Park, Y.; Cheon, B.; Park, M. H. Carbon Dots as an Effective Fluorescent Sensing Platform for Metal Ion Detection. *Nanoscale Res. Lett.* **2019**, *14*, 272.

(24) Li, P.; Li, S. F. Y. Recent advances in fluorescence probes based on carbon dots for sensing and speciation of heavy metals. *NANO* **2021**, *10*, 877−908.

(25) El-Shafey, A. M. Carbon dots: Discovery, structure, fluorescent properties, and applications. *Green Process. Synth.* **2021**, *10*, 134−156.

(26) Sekar, A.; Yadav, R.; Basavaraj, N. Fluorescence quenching mechanism and the application of green carbon nanodots in the detection of heavy metal ions: a review. *New J. Chem.* **2021**, *45*, 2326−2360.

(27) Nazri, N. A. A.; Azeman, N. H.; Luo, Y.; Bakar, A. A. A. Carbon quantum dots for optical sensor applications: A review. *Opt. Laser Technol.* **2021**, *139*, 106928.

(28) Ghanem, A.; Al-Qassar Bani Al-Marjeh, R.; Atassi, Y. Novel nitrogen-doped carbon dots prepared under microwave-irradiation for highly sensitive detection of mercury ions. *Heliyon* **2020**, *6*, No. e03750.

(29) Ye, Z.; Zhang, Y.; Li, G.; Li, B. Fluorescent Determination of Mercury(II) by Green Carbon Quantum Dots Synthesized from Eggshell Membrane. *Anal. Lett.* **2020**, *53*, 2841−2853.

(30) Omer, K. M.; Hama Aziz, K. H.; Mohammed, S. J. Improvement of selectivity via the surface modification of carbon nanodots towards the quantitative detection of mercury ions. *New J. Chem.* **2019**, *43*, 12979−12986.

(31) Yahyazadeh, E.; Shemirani, F. Easily synthesized carbon dots for determination of mercury(II) in water samples. *Heliyon* **2019**, *5*, No. e01596.

(32) Mohammadpour, Z.; Safavi, A.; Shamsipur, M. A new label free colorimetric chemosensor for detection of mercury ion with tunable dynamic range using carbon nanodots as enzyme mimics. *Chem. Eng. J.* **2014**, *255*, 1−7.

(33) Pajewska-Szmyt, M.; Buszewski, B.; Gadzala-Kopciuch, R. Carbon dots as rapid assays for detection of mercury(II) ions based on turn-off mode and breast milk. *Spectrochim. Acta, Part A* **2020**, *236*, 118320.

(34) Tadesse, A.; Hagos, M.; RamaDevi, D.; Basavaiah, K.; Belachew, N. Fluorescent-Nitrogen-Doped Carbon Quantum Dots Derived from Citrus Lemon Juice: Green Synthesis, Mercury(II) Ion Sensing, and Live Cell Imaging. *ACS Omega* **2020**, *5*, 3889−3898.
(35) Zhang, Q.; Zhang, X.; Bao, L.; Wu, Y.; Jiang, L.; Zheng, Y.; Wang, Y.; Chen, Y. The Application of Green-Synthesis-Derived Carbon Quantum Dots to Bioimaging and the Analysis of Mercury(II). *J. Anal. Methods Chem.* **2019**, *2019*, 8183134.
(36) Qu, S.; Wang, X.; Lu, Q.; Liu, X.; Wang, L. A biocompatible fluorescent ink based on water-soluble luminescent carbon nanodots. *Angew. Chem., Int. Ed.* **2012**, *51*, 12215−12218.
(37) Qin, X.; Lu, W.; Asiri, A. M.; Al-Youbi, A. O.; Sun, X. Microwave-assisted rapid green synthesis of photoluminescent carbon nanodots from flour and their applications for sensitive and selective detection of mercury(II) ions. *Sens. Actuators, B* **2013**, *184*, 156−162.
(38) Sk, M. P.; Chattopadhyay, A. Induction coil heater prepared highly fluorescent carbon dots as invisible ink and explosive sensor. *RSC Adv.* **2014**, *4*, 31994−31999.
(39) Han, Z.; He, L.; Pan, S.; Liu, H.; Hu, X. Hydrothermal synthesis of carbon dots and their application for detection of chlorogenic acid. *Luminescence* **2020**, *35*, 989−997.
(40) Bajpai, S. K.; D'Souza, A.; Suhail, B. Blue light-emitting carbon dots (CDs) from a milk protein and their interaction with Spinacia oleracea leaf cells. *Int. Nano Lett.* **2019**, *9*, 203−212.
(41) Fu, Y.; Zhao, S.; Wu, S.; Huang, L.; Xu, T.; Xing, X.; Lan, M.; Song, X. A carbon dots-based fluorescent probe for turn-on sensing of ampicillin. *Dyes Pigm.* **2020**, *172*, 107846.
(42) Li, X.; Zhang, S.; Kulinich, S. A.; Liu, Y.; Zeng, H. Engineering surface states of carbon dots to achieve controllable luminescence for solid-luminescent composites and sensitive Be^{2+} detection. *Sci. Rep.* **2014**, *4*, 4976.
(43) Hoan, B. T.; Van Huan, P.; Van, H. N.; Nguyen, D. H.; Tam, P. D.; Nguyen, K. T.; Pham, V. H. Luminescence of lemon-derived carbon quantum dot and its potential application in luminescent probe for detection of $Mo^{(6+)}$ ions. *Luminescence* **2018**, *33*, 545−551.
(44) Wang, C.; Hu, T.; Wen, Z.; Zhou, J.; Wang, X.; Wu, Q.; Wang, C. Concentration-dependent color tunability of nitrogen-doped carbon dots and their application for iron(III) detection and multicolor bioimaging. *J. Colloid Interface Sci.* **2018**, *521*, 33−41.
(45) Liu, W.; Diao, H.; Chang, H.; Wang, H.; Li, T.; Wei, W. Green synthesis of carbon dots from rose-heart radish and application for Fe^{3+} detection and cell imaging. *Sens. Actuators, B* **2017**, *241*, 190−198.
(46) Askarinejad, A.; Morsali, A. Synthesis and characterization of mercury oxide unusual nanostructures by ultrasonic method. *Chem. Eng. J.* **2009**, *153*, 183−186.
(47) Tang, Q.; Zhu, W.; He, B.; Yang, P. Rapid Conversion from Carbohydrates to Large-Scale Carbon Quantum Dots for All-Weather Solar Cells. *ACS Nano* **2017**, *11*, 1540−1547.
(48) Wei, X.-M.; Xu, Y.; Li, Y.-H.; Yin, X.-B.; He, X.-W. Ultrafast synthesis of nitrogen-doped carbon dots via neutralization heat for bioimaging and sensing applications. *RSC Adv.* **2014**, *4*, 44504−44508.
(49) Zhao, C.; Li, X.; Cheng, C.; Yang, Y. Green and microwave-assisted synthesis of carbon dots and application for visual detection of cobalt(II) ions and pH sensing. *Microchem. J.* **2019**, *147*, 183−190.
(50) Edison, T. N.; Atchudan, R.; Sethuraman, M. G.; Shim, J. J.; Lee, Y. R. Microwave assisted green synthesis of fluorescent N-doped carbon dots: Cytotoxicity and bio-imaging applications. *J. Photochem. Photobiol., B* **2016**, *161*, 154−161.
(51) Barati, A.; Shamsipur, M.; Arkan, E.; Hosseinzadeh, L.; Abdollahi, H. Synthesis of biocompatible and highly photoluminescent nitrogen doped carbon dots from lime: analytical applications and optimization using response surface methodology. *Mater. Sci. Eng., C* **2015**, *47*, 325−332.
(52) Kuzmenko, V.; Naboka, O.; Staaf, H.; Haque, M.; Göransson, G.; Lundgren, P.; Gatenholm, P.; Enoksson, P. Capacitive effects of nitrogen doping on cellulose-derived carbon nanofibers. *Mater. Chem. Phys.* **2015**, *160*, 59−65.
(53) Shah, H.; Xin, Q.; Jia, X.; Gong, J. R. Single precursor-based luminescent nitrogen-doped carbon dots and their application for iron (III) sensing. *Arabian J. Chem.* **2019**, *12*, 1083−1091.
(54) He, J. H.; Cheng, Y. Y.; Yang, T.; Zou, H. Y.; Huang, C. Z. Functional preserving carbon dots-based fluorescent probe for mercury (II) ions sensing in herbal medicines via coordination and electron transfer. *Anal. Chim. Acta* **2018**, *1035*, 203−210.
(55) Yan, F.; Kong, D.; Luo, Y.; Ye, Q.; He, J.; Guo, X.; Chen, L. Carbon dots serve as an effective probe for the quantitative determination and for intracellular imaging of mercury(II). *Microchim. Acta* **2016**, *183*, 1611−1618.
(56) Li, L.; Yu, B.; You, T. Nitrogen and sulfur co-doped carbon dots for highly selective and sensitive detection of Hg (II) ions. *Biosens. Bioelectron.* **2015**, *74*, 263−269.
(57) U.S. Food and Drug Administration. *Prohibited & Restricted Ingredients in Cosmetics*.; U.S. Food and Drug Administration https://www.fda.gov/cosmetics/cosmetics-laws-regulations/prohibited-restricted-ingredients-cosmetics. (accessed 2022-12-13).
(58) Codex Alimentarius Commission. *CAC/GL 40−1993 Guidelines on Good Laboratory Practice in Pesticide Residue Analysis*; Codex Alimentarius Commission: Rome, Italy: 2010.
(59) AOAC International. *AOAC SMPR 2012.007 Standard Method Performance Requirements for Heavy Metals in a Variety of Foods and Beverages*; AOAC International: Rockville, USA: 2021.
(60) Agilent Technologies, I. *Multi-element calibration standard-2A*.; Agilent Technologies, I. https://www.agilent.com/store/en_US/Prod-8500-6940/8500-6940 . (accessed 2022-12-10).
(61) Liu, J.; Li, R.; Yang, B. Carbon Dots: A New Type of Carbon-Based Nanomaterial with Wide Applications. *ACS Cent. Sci.* **2020**, *6*, 2179−2195.

https://doi.org/10.1021/acsomega.2c07175
ACS Omega 2023, 8, 7615−7625